MICROWAVE CHARACTERISTICS OF PLANAR ELECTROOPTIC MODULATOR

R. DELRUE, E. PALECZNY, J.F. LEGIER, P. PRIBETICH, P. KENNIS

CENTRE HYPERFREQUENCES ET SEMICONDUCTEURS, Equipe Electromagnétisme des Circuits
U.A. CNRS n° 287, U.S.T.L. Flandres Artois, 59655 Villeneuve d'Ascq Cedex - France

ABSTRACT

We present in this communication an attempt to modelize new travelling wave optical modulators in the microwave frequency range by two methods : a desktop computer one based on the effective complex dielectric constant and a more rigourous method : the mode matching technique.

INTRODUCTION

Electrooptic waveguide modulators with high frequency drive capability and moderate operating voltages are important components in high speed optical communications. Devices in III-V semiconductors are of growing interest because they have the potential of monolithic integration into electronic circuits, lasers and detectors.

Different types of modulator have been developed :
- Integrated Mach Zehnder interferometers [1] (they allow amplitude, frequency and phase modulations.
- Directional couplers (they can be used either as modulators or as switchers) [2].

In order to achieve higher bandwidth than lithium niobate modulators, high optical power density and monolithic integrability, p.i.n. microstrip modulators have been proposed but high microwave losses and slowing effects [3], [5] do not allow efficient optical modulation despite of a nearly 100% overlap of the optical field and the electric field. Some authors [4] have proposed new topologies (figure 1) as good candidates for single pass travelling wave modulator. In fact, the design of such devices which couple microwave and optical signal needs to characterize both the behaviour of the structure in the optical frequency range and in the microwave frequency range. The purpose of this communication is to quantify both bulk microwave losses and metallic ones but also to determine the phase velocity in the microwave frequency range. This study is made by taking into account the geometry of the cross section of the structure, the multilayered nature of waveguide and the hybrid nature of the mode.

NUMERICAL STUDY

The aim of the numerical simulation of the structure in the microwave frequency range is to obtain propagation characteristics necessary to evaluate the efficiency of the single pass travelling wave electrooptic modulator. The structure figure 1-a is a dielectric loaded optical guide single mode at 1.3μm with symmetric coplanar strip electrodes plated with one electrode crossing over the guide.

The rf and dc applied electric fields are parallel to the <100> crystal axis. The structure figure 1-b is a ridge optical guide single mode with symmetric coplanar strip electrodes on either side of the guide resulting in the applied electric field parallel to the <011> direction. In order to simulate the microwave structures, we must consider modelized structures. The figure 2 shows the models. In a first step, we have focused our attention on the structure 2.b. Two parallel studies have been developped : a rigourous one which is the mode matching technique and a classical approached method which can be easily implemented on a desktop-computer : the method of the effective complex dielectric constant.

THE BASIC STRUCTURE AND THE METHODS OF ANALYSIS

The basic structure

The investigated waveguide structure is shown on figure 3. As we can see, the cross section located in the xoy plane is composed with seven regions which are noted 0, 1, 2, 1', 3, 4, 5 with different complex permittivity ε^*_0, ε^*_1, $\varepsilon^*_{1'}$, ε^*_2, ε^*_3, ε^*_4, ε^*_5. As we want a generalized formulation, the vertical plane ($Y = h_2$) can be considered as an electric or magnetic wall according with the studied propagated mode of the waveguide.

The reference method of analysis : the Mode Matching Technique

The method used to calculate the complex

1989 IEEE MTT-S Digest

phase constant $\gamma_z = \alpha_z + jK_z$ is the well known Mode Matching one, which has been used by several authors these last years [6]. A complete set of field solutions is derived for each subdomain "i" of complex permittivity constant $\varepsilon^*_i = \varepsilon'_i - j\varepsilon''_i$. It is assumed that the dependance of the whole field components refered to the z coordinate, can be expressed as a function of exp $(-\gamma_z)$, γ_z being the complex longitudinal propagation constant previously mentioned. All the x and y dependance of the fields is formulated using harmonics functions excepted in region I where the x field behaviour is given by an exponential decay. So, the electric and magnetic field potential expansions respectively ψ_y, ϕ_y, can be written, according to the boundary conditions on the magnetic or electric walls at $y = h_2$, $y = 0$ et $x = -L_5$, as followed :

Subdomain 0

$$(1)\quad \psi_y^{(0)} = \sum_{n=0}^{N} A_n \exp\left(-K_{xn}^{(0)}(x+L_1)\right) \cos K_{yn}^{(0)} y$$

$$(2)\quad \phi_y^{(0)} = \sum_{m=0}^{M} B_m \exp\left(-\tilde{K}_{xm}^{(0)}(x+L_1)\right) \sin \tilde{K}_{ym}^{(0)} y$$

Subdomain 1

$$(3)\quad \psi_y^{(1)} = \sum_{n=1}^{N} \left(C_n \sin K_{xn}^{(1)} x + C'_n \cos K_{xn}^{(1)} x\right) \cos K_{yn}^{(1)} y$$

$$(4)\quad \phi_y^{(1)} = \sum_{m=1}^{M} \left(D_m \sin \tilde{K}_{xm}^{(1)} x + D'_m \cos \tilde{K}_{xm}^{(1)} x\right) \sin \tilde{K}_{ym}^{(1)} y$$

Subdomain 2 for electric wall

$$(5)\quad \psi_y^{(2)} = \sum_{n=1}^{N} \left(E_n \sin K_{xn}^{(2)} x + E'_n \cos K_{xn}^{(2)} x\right) \cos K_{yn}^{(2)} y$$

$$(6)\quad \phi_y^{(2)} = \sum_{m=1}^{M} \left(F_n \sin \tilde{K}_{xm}^{(2)} x) + F'_n \cos \tilde{K}_{xm}^{(2)} x\right) \sin \tilde{K}_{ym}^{(2)} y$$

Subdomain 2 for magnetic wall

$$(5)\quad \psi_y^{(2)} = \sum_{n=1}^{N} \left(E_n \sin K_{xn}^{(2)} x + E'_n \cos K_{xn}^{(2)} x\right) \sin K_{yn}^{(2)} y$$

$$(6')\quad \phi_y^{(2)} = \sum_{m=1}^{M} \left(F_n \sin \tilde{K}_{xm}^{(2)} x + F'_n \cos \tilde{K}_{xm}^{(2)} x\right) \cos \tilde{K}_{ym}^{(2)} y$$

Subdomain i (i=1',3,4)

$$(7)\quad \psi_y^{(i)} = \sum_{n=1}^{N} \left(G_n \sin K_{xn}^{(i)} x + G'_n \cos K_{xn}^{(i)} x\right) \cos K_{yn}^{(i)} y$$

$$(8)\quad \phi_y^{(i)} = \sum_{m=1}^{M} \left(H_m \sin \tilde{K}_{xm}^{(i)} + H'_m \cos \tilde{K}_{xm}^{(i)} x\right) \sin \tilde{K}_{ym}^{(i)} y$$

Subdomain 5

$$(9)\quad \psi_y^{(5)} = \sum_{n=0}^{N} I_n \sin K_{xn}^{(5)} (x+L_5) \cos K_{yn}^{(5)} y$$

$$(10)\quad \phi_y^{(5)} = \sum_{m=0}^{M} J_m \cos \tilde{K}_{xm}^{(5)} (x+L_5) \sin \tilde{K}_{ym}^{(5)} y$$

In equation (1) to (10), $Kx^{(i)}$ and $Ky^{(i)}$ are the complex wave numbers of the TM^Y modes and $\tilde{K}x(i)$, $\tilde{K}y(i)$ those of the corresponding TE^Y modes in the different subarea. These equations describe a complete solution for the fields if N and M become infinite. From the continuity relations in the different plane $x = \pm L_1$, $y = 0$ and $y = h_2$, we obtained a complete set of relations which must be numerically solved in complex domain.

The method of the effective complex dielectric constant (ECDC)

The effective dielectric constant approximation is actually quite an old one, but it is a very simple and practical method for obtaining reasonably accurate values of kz for a wide range of dielectric waveguide structures as Toulios, Itoh and other authors have shown it [7], [8], [9], [10], in the lossless case.

So, it has seemed interesting by comparison with MMT to evaluate the potentiality of this method in the determination of the attenuation α_z and the propagation constant K_z of lossy dielectric waveguide via the calculus of an effective complex dielectric constant.

NUMERICAL RESULTS

After the classical tests on lossless structures, we present figure 4 a comparison between ECDC and Mode Matching results for moderate lossy structures. For such cases, the two methods give quite similar results.
However, when more realistic structures with high doped multilayered substrate are considered, only rigourous method (Mode Matching for example) can be used. In this mind, we present, figure 5 the frequency behaviours of the attenuation constant and the phase velocity in the microwave frequency range of the structure 2-b for several sets of geometrical and physical parameters. As example, in the proceeding, we have only presented the limit case when the studied structure 2-b is not depleted and so exhibit the maximum losses and slowing factor due to the presence of the multilayered doped substrate. Note that in this case, the microwave phase velocity is yet much lower than the optical phase velocity and so induce mismatching between optical and microwave signals.

CONCLUSION

We have presented in this communication a first step of the modelization of new travelling wave optical modulators by two kinds of methods : a desktop computer one (the method of the effective complex dielectric constant) which is an approximate modelization but simple and a more rigourous method : the Mode Matching Technique. However, at this time, the validity of the results obtained by the Mode Matching Technique as compared to the experimental ones are conditionned by the choice of the model of the structure. The next steps of the study will include more realistic model taking into account the air gaps between the electrodes and the rib structure. So, with such improvements, we shall study with accuracy, the influence of the doping level of each semiconductor layers, as the influence of different bias voltage values.

REFERENCE

[1] P. BUCHMAN, H. KAUFMANN, H. MELCHIOR, G. GUEKOS : "Broadband Y. branch Electrooptic GaAs Waveguide Interferometer for 1.3μm", Appl. Phys. Lett., 46, p.462 (1985)

[2] P. BUCHMAN, H. KAUFMANN, H. MELCHIOR, G. GUEKOS :"Gallium arsenide waveguide interferometers and couplers for high speed electrooptic modulation and switching", Proceedings of Symposium on Optical and Electro-optical Applied Sciences and Engineering, Cannes, November 1985, p.567.
[3] S.H. LIN, S.Y. WANG, Y.M. HOUNG : "GaAs pin electro-optic travelling-wave modulator at 1.3µm", Electronics Letters, August 1986, vol. 22, n°18, pp. 934-935.
[4] S.Y. WANG, S.H. LIN, Y.M. YOUNG : "GaAs travelling wave polarization electro-optic waveguide modulator with band-width in excess of 20GHz at 1.3µm", Appl. Phys. Lett. 51 (2), July 1987, pp. 83-85.
[5] D. REMIENS, P. PRIBETICH, P. KENNIS, C. SEGUINOT : "Microwave performance prediction of a III-V semiconductor electrooptic waveguide modulator", Applied Optics, vol. 26, January 1987, pp. 118-120.
[6] B. YOUNG, T. ITOH : "Los reduction in superconducting microstrip line transmission lines", IEEE M.T.T. Symposium Digest, New York, June 1988 pp. 453-456.
[7] R.M. KNOX and P.P. TOULIOS : "Integrated circuits for the millimeter wave through optical frequency range", in Proc. Symp. Submillimeter Waves, Brooklyn, NY : Polytechnic Press, Apt. 1970, pp. 497-516.
[8] W.V. McLEVIGE, T. ITOH and R. MITTRA : "New Waveguide structures for millimeter-wave and optical integrated circuits", IEEE Trans. Microwave Theory Tech., vol. MTT-23, pp. 788-794, Oct. 1975.
[9] T. ITOH : "Inverted strip dielectric waveguide for millimeter-wave integrated circuits", IEEE Trans. Microwave Theory Tech., vol. MTT-24, pp. 821-827, Nov. 1976.
[10] Arthur A. OLINER, SONG-TSUEN PENG, TING-IH-HSU, Alberto SANCHEZ : "Guidance and Leakage properties of a class of open dielectric waveguides" : part I and part II. New physical effects, IEEE MTT, september 1981.

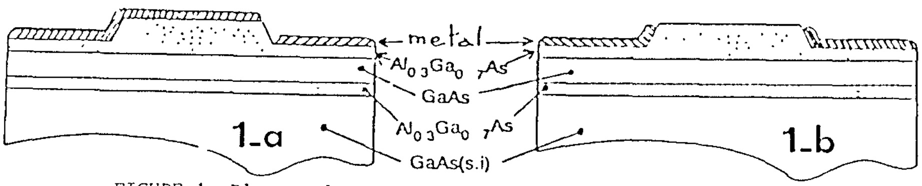

FIGURE 1: Planar electrooptic modulator topologies

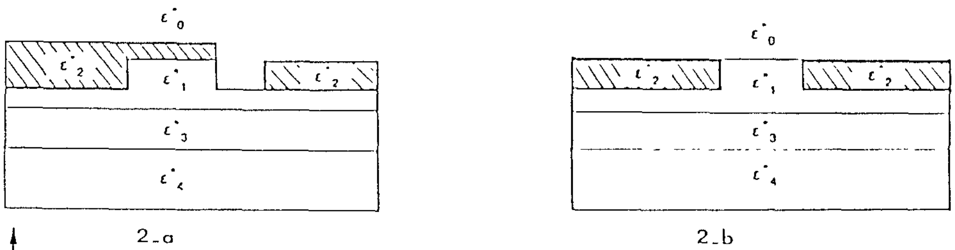

FIGURE 2: Models of the studied planar electrooptic modulators

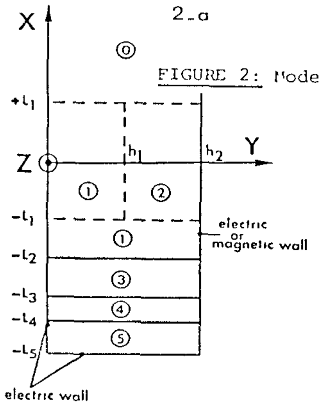

FIGURE 3: The generalized studied structure

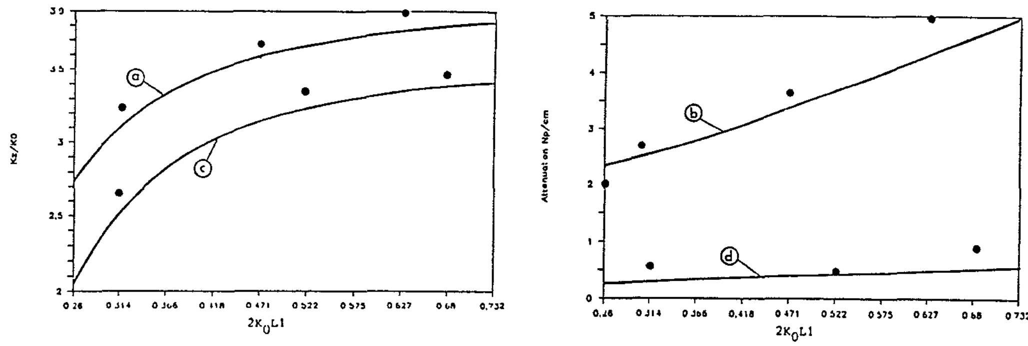

Figure 4 . Dispersion characteristics for lossy rib waveguide versus the normalized frequency $2k_0L_1$ ($k_0 = \omega/c$)

$\varepsilon_i = \varepsilon_0 (\varepsilon'_{ri} - j\,\varepsilon''_{ri})$

$\varepsilon'_{r0} = \varepsilon'_{r1} = 1 \quad \varepsilon''_{r0} = \varepsilon''_{r1} = 0$

$\varepsilon'_{r2} = \varepsilon'_{r1'} = \varepsilon'_{r3} = \varepsilon'_{r4} = \varepsilon'_{r4} = \varepsilon'_{r5} = 13$

$(L_5 - L_1)/2L_1 = 1$

$h_2/(h_2 - h_1) = 3{,}8$

$h_2 - h_1 = 4L_1$

4.a. Microwave Normalized phase constant $\varepsilon''_{r2} = \varepsilon''_{r1'} = \varepsilon''_{r3} = \varepsilon''_{r4}$

4.b. Microwave attenuation constant $\varepsilon''_{r4} = \varepsilon''_{r5} = 13$

4.c : Microwave normalized phase constant $\varepsilon''_{r2} = \varepsilon''_{r1'} = \varepsilon''_{r3} = \varepsilon''_{r4}$

4.d : Microwave attenuation constant $\varepsilon''_{r4} = \varepsilon''_{r5} = 0.13$

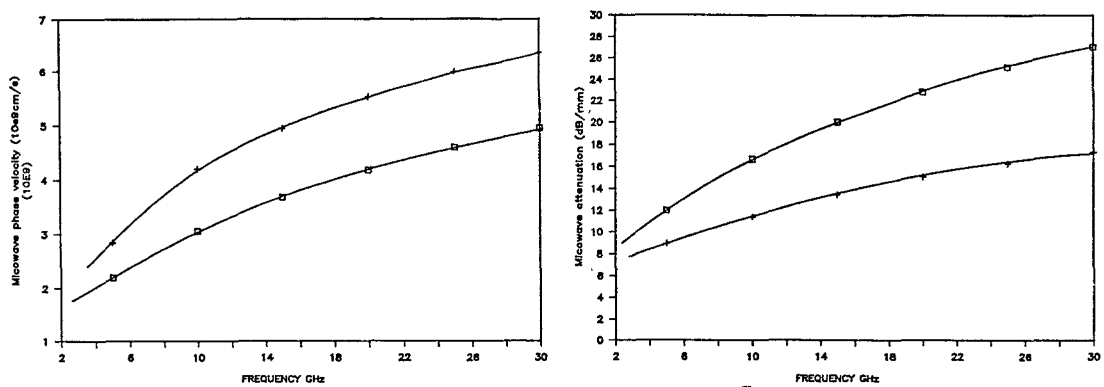

Figure 5 : Frequency behaviour of Microwave characteristics

5.a. Microwave phase velocity

5.b. Microwave Attenuation constant

$L_1 = 0{,}25\mu m$, - $L_1 = 0{,}25\mu m$, - $L_2 = 0{,}75\mu m$, - $L_3 = 1{,}75\mu m$, - $L_4 = 3{,}75\ \mu m$, - $L_5 = 100\mu m$

$h_1 = 60\mu m$, $h_2 == 62{,}5\mu$, $\varepsilon_{r0} = 1$, $\varepsilon_{r2} = 12{,}2$, $\varepsilon_{r1'} = 12{,}2$, $\varepsilon_{r3} = 13{,}1$, $\varepsilon_{r4} = 12{,}2$, $\varepsilon_{r5} = 13{,}1$

□: $N_{D2} = 10^{16} At/cm3$, $N_{D1'} = 10^{16} At/cm3$, $N_{D3} = 10^{13} At/cm3$, $N_{D4} = 10^{16} At/cm3$.

+: $N_{D2} = 10^{15} At/cm3$, $N_{D1'} = 10^{15} At/cm3$, $N_{D3} = 10^{15} At/cm3$, $N_{D4} = 10^{15} At/cm3$.